



CHORUS

This is the accepted manuscript made available via CHORUS. The article has been published as:

Maximum mass and radius of neutron stars, and the nuclear symmetry energy

S. Gandolfi, J. Carlson, and Sanjay Reddy

Phys. Rev. C **85**, 032801 — Published 9 March 2012

DOI: [10.1103/PhysRevC.85.032801](https://doi.org/10.1103/PhysRevC.85.032801)

The maximum mass and radius of neutron stars and the nuclear symmetry energy

S. Gandolfi,¹ J. Carlson,¹ and Sanjay Reddy^{1,2}

¹*Theoretical Division, Los Alamos National Laboratory, Los Alamos, NM 87545, USA*

²*Institute for Nuclear Theory, University of Washington, Seattle, WA 98195-1550, USA*

We calculate the equation of state of neutron matter with realistic two- and three-nucleon interactions using Quantum Monte Carlo techniques, and illustrate that the short-range three-neutron interaction determines the correlation between neutron matter energy at nuclear saturation density and higher densities relevant to neutron stars. Our model also makes an experimentally testable prediction for the correlation between the nuclear symmetry energy and its density dependence - determined solely by the strength of the short-range terms in the three neutron force. The same force provides a significant constraint on the maximum mass and radius of neutron stars.

PACS numbers: 21.65.Cd, 21.65.Ef, 26.60.-c, 26.60.Kp

Since their discovery, neutron stars have remained our sole laboratory to study matter at supra-nuclear density and relatively low temperature. The equation of state (EoS) of matter at these densities is largely unknown, but uniquely determines the structure of neutron stars and the relation between their mass (M) and radius (R). Matter that can support large pressure for a given energy density (typically called a stiff EoS), will favor large neutron star radii for a given mass. Such EoS also predict large values for the maximum mass of a neutron star stable with respect gravitational collapse to a black hole. Conversely, a high density phase that predicts a smaller pressure will result in more compact neutron stars and smaller maximum masses.

The recent accurate measurement of a large neutron star mass $M = 1.97 \pm 0.04 M_{\text{Solar}}$ in the system called J1614-2230 provides strong evidence that the high density equation of state is stiff [1]. Interestingly, attempts to infer neutron star radii have favored relatively small values ranging from 9 – 12 km [2–4]. Although the radius inference depends on specific model assumptions, these smaller radii imply a soft EoS in the vicinity of nuclear saturation density. Taken together, they indicate that the EoS of dense matter makes a transition from soft to stiff at supra-nuclear density. In this article we show that the 3-neutron force (3n) is the key microscopic ingredient that determines the nature of this transition.

The importance of 3 body forces in nuclear physics is well known, and Quantum Monte Carlo (QMC) calculations of light nuclei have clarified its structure and strength. However, in these systems the dominant 3 body force acts between two neutrons and proton or between two protons and a neutron. While the force between 3 neutrons (3n) is important in light neutron-rich nuclei, the short distance behavior is not easily accessible [5]. Properties of large neutron-rich nuclei are potentially sensitive to this interaction, especially if the symmetry energy provides a reliable measure of the energy difference between pure neutron matter and symmetric nuclear matter at saturation density. There has been much recent progress in both theory and experiments to measure the symmetry energy and its density dependence as reviewed in Ref. [6, 7]. The symmetry energy is expected to

be in the range 32 ± 2 MeV. We explore this experimentally suggested range for the nuclear symmetry energy and show that a more precise determination is needed to adequately constrain the 3n interaction.

In this work we solve the non-perturbative many-body nuclear Hamiltonian using the Auxiliary Field Diffusion Monte Carlo [8] method. Its accuracy in studying nuclear systems has been tested in light nuclei [9]. The extension to include three-body forces in pure neutron rich systems is straightforward with no additional approximations within the AFDMC technique [10], and a comparison with the Green's function Monte Carlo (GFMC) has been extensively tested in neutron drops [11]. We present results for the EoS of neutron matter using phenomenological 2-neutron (2n) potentials which provide an accurate description of nucleon-nucleon scattering data up to high energies, and study the role of the poorly constrained 3n interaction.

In earlier work it has been established that the EoS in the density regime $1 - 3 \rho_0$ plays an essential role in determining the neutron star radius [12]. In this density regime, the 3n interaction plays a critical role because of a large cancellation between the attractive and repulsive parts of the 2n interaction arising from the long and short distance behavior, respectively. Consequently, we find that the neutron star radius for a canonical mass of $1.4 M_{\text{Solar}}$ is especially sensitive to the 3n interaction. Although matter in the neutron star will contain a small admixture of protons, here we calculate the EoS of pure neutron matter for the following reasons. First, the structure of the interactions between neutrons is simpler than those between neutron and protons. Second, these simpler interactions are amenable to QMC methods to solve the many-body problem as it is devoid of the complexities of the isospin dependent spin-orbit and three-nucleon potentials, and clustering effects likely in systems with protons. Third, the fraction of protons required to ensure stability is small and is typically less than 10%. Finally, since generically neutron matter has higher pressure than matter containing any fraction of protons or strangeness in the form of hyperons or kaons, our results provide stringent upper bounds on the neutron maximum mass and radius.

To compute the EoS for neutron stars it is necessary to describe the nucleon-nucleon interactions at short-distances or large relative momenta up to $p \simeq 2p_{Fn} \simeq 660 \text{ MeV}(\rho/\rho_0)^{1/3}$ where p_{Fn} is the Fermi momentum, ρ is density in the typical density in the neutron star core and $\rho_0 = 0.16 \text{ fm}^{-3}$ is the nuclear saturation density. Relative momenta up to p_{Fn} are required in even a mean-field (Fermi gas) description, and the nn interaction scatters nucleons to larger momenta up to of order 1.5 to 2 p_{Fn} at saturation density. Descriptions of higher density neutron matter with softer interactions if they are consistently evolved to lower scales, including induced 3n (and potentially 4n) interactions.

Phenomenological two nucleon potentials such as the Argonne potential have been constructed to describe scattering data up to relative momenta $\simeq 600 \text{ MeV}$ with high accuracy [13]. Despite the fact that the Argonne potential has been fit up to lab energies of 350 MeV, it very well reproduces scattering data up to much larger energies [14]. The AV8' interaction we employ in this study is identical to the full AV18 interaction in s - and p -waves, and includes the dominant one-pion interaction in higher partial waves. Chiral interactions also reproduce the scattering data very well below 350 MeV lab energy, but fail rapidly above because of the cutoff in presently-available interactions. At larger momentum transfer, the potentials cannot describe inelasticities but in scattering channels where inelasticities are known to be small they have been shown to provide a good description. They also provide good predictions [15] of high-momentum components of nuclear wave functions as observed in nucleon [16, 17] and electron scattering [18, 19]. These high momentum observables provide a test of the assumed short-distance features. In the low-energy high-momentum region relevant to neutron stars the inelasticities in 2n scattering must be absorbed into many-body forces (3n, 4n, ...) intimately connected to the short-distance behavior of the 2n interaction.

The nuclear Hamiltonians we consider contain the non-relativistic kinetic energy, and the 2n and 3n interactions:

$$H = -\frac{\nabla^2}{2m} + V_{2n} + V_{3n}. \quad (1)$$

For the 2n potential, we use the Argonne AV8' model [20] and the form of the 3n interaction is inspired by both the Urbana IX and the Illinois models [5]. We consider a range of 3n interactions that contain long-distance s - and p -wave 2π exchange contributions, an intermediate range (3π loops) contribution, and a spin-independent short-range repulsive term. Explicitly,

$$V_{3N} = A_{2\pi}^{PW} \mathcal{O}^{2\pi, PW} + A_{2\pi}^{SW} \mathcal{O}^{2\pi, SW} + A_{3\pi} \mathcal{O}^{3\pi} + A_R \mathcal{O}^R. \quad (2)$$

This form of interaction includes all the terms present in low order chiral interaction, plus selected terms found to be important in studies of light nuclei and nuclear matter using the Argonne interactions.

The structure of the operators \mathcal{O} appearing above are defined in Ref. [5]. The relative contributions of these

four components of the 3n force depends on the 2n interaction. We find that for the Argonne potential, the 2n interactions suppress the long-distance (2π) contribution of the 3n force in the ground state. This suppression is a result of the pion-range correlations induced by the 2n force, we find it also occurs for the Super-Soft Core NN interaction [21]. For typical range of values of the strength parameter $A_{2\pi}^{PW}$ and $A_{2\pi}^{SW}$ considered in Ref. [5] we find the contribution of these operators to the ground state energy is repulsive but very small at all densities studied. In contrast, this interaction is large and attractive in light nuclei where both neutrons and protons contribute. The intermediate-range (3π) 3n interaction was introduced to fit the properties of weakly-bound neutron-rich nuclei like ${}^8\text{He}$ [5]. Earlier calculations [10] have shown that this interaction is strong and attractive in neutron matter for typical values of $A_{3\pi}$ quoted in Ref. [5]. In this work, we explored a range of values for $A_{3\pi}$ ranging from zero to that in the Illinois-7 3n interaction [22] because the structure of this term is still not fully understood or constrained. We use a phenomenological short-range repulsive term as in the Urbana and Illinois three-body forces, with $V_R = A_R \mathcal{O}^R = A_R \sum_{cyc} T^2(m_\pi r_{ij}) T^2(m_\pi r_{jk})$, where the function $T(x)$ is defined in Ref. [5]. We have also considered a different form $V_\mu^R = A_R \sum_{cyc} v(r_{ij}) v(r_{jk})$ with and $v(r) = \exp(-2\mu r)$; other different forms of V_R have been explored, giving very similar results.

The 3n interaction we employ is not intended to be a microscopic treatment of the complete 3n interaction. It assumes that for the neutron matter equation of state the effects of more complicated spin-dependent short-distance 3n interactions, relativistic effects, and potential 4n interactions can be mimicked with simplified three-neutron interactions with a wide range of spatial dependence. This assumption has been tested in the case of relativistic corrections, where Ref. [23] find that the density dependence of the relativistic effects are similar to the 3n interaction. Further tests of the density dependence of specific higher-order terms in the chiral interaction are valuable. The different forms of V_R we have explored span a wide range of density dependence for the 3n interaction, as shown below.

For the 3n interaction we vary both $A_{3\pi}$ and μ to study the sensitivity to short-range physics. The strength of the short-range 3n interaction A_R is taken to be a free parameter adjusted to yield the experimentally accessible nuclear symmetry energy. Although not proven, we make the following reasonable assumptions: 1) relativistic effects in neutron matter show a similar density dependence to the short-range three-nucleon interaction as carefully studied in Ref. [23], 2) the density dependence of additional spin-dependent short-range 3n interactions (for example higher-order terms in chiral expansions) in the equation of state of neutron matter can be described in a spin-independent model, and 3) four-nucleon force contributions with different density dependence are suppressed relative to the 3n force for densities up to 2 – 3

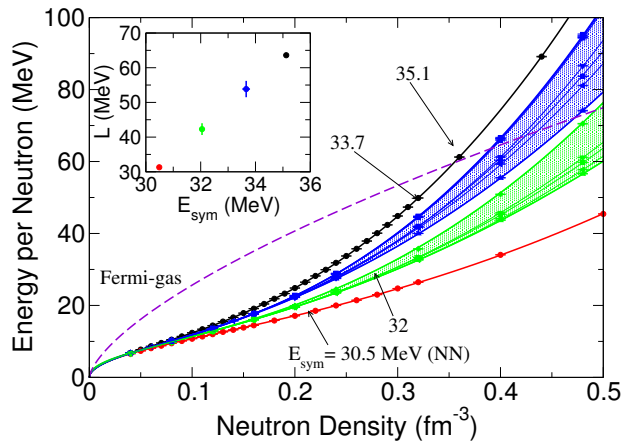


FIG. 1. (Color online) The energy per particle of neutron matter for different values of the nuclear symmetry energy (E_{sym}). For each value of E_{sym} the corresponding band shows the effect of different spatial and spin structures of the three-neutron interaction. The inset shows the linear correlation between E_{sym} and its density derivative L .

ρ_0 . This assumption can be justified at nuclear density by the high precision fits to light-nuclei obtained with only 3n forces [24], at higher density this model assumption can be tested by its predicted correlation between properties of neutron-rich nuclei and neutron stars.

We assume that $E_{\text{sym}} = E_{\text{neutron}}(\rho_0) - E_{\text{nuclear}}(\rho_0)$ and using experimental values of $E_{\text{sym}} = 32 \pm 2$ MeV [25] and $E_{\text{nuclear}}(\rho_0) = -16.0 \pm 0.1$ MeV from nuclear masses models [26] obtain an empirical constraint for neutron matter energy $E_{\text{neutron}}(\rho_0) = 16 \pm 2$ MeV. Potential higher-order corrections to the quadratic nuclear symmetry energy, for which there is some theoretical motivation but no clear experimental evidence, may affect the extraction of the neutron matter energy and increase the associated error. In this work we ignore these poorly known corrections and tune A_R to reproduce the neutron matter energy in the range 16 ± 2 MeV. Our results are shown in Fig. 1, where the green and blue points are QMC results for different choices of A_R corresponding to $E_{\text{neutron}}(\rho_0) = 16$ MeV ($E_{\text{sym}} = 32$ MeV) and $E_{\text{neutron}}(\rho_0) = 17.7$ MeV ($E_{\text{sym}} = 33.7$ MeV), respectively. The results are compared to those obtained using a 2n force without 3n ($E_{\text{sym}} = 30.5$ MeV), and 2n combined with the Urbana IX 3n ($E_{\text{sym}} = 35.1$ MeV). The bands depict the sensitivity to short-distance spin and spatial structure of the 3n interaction and are obtained by varying the range of the 3n short-distance force and $A_{3\pi}$.

In the vicinity of nuclear density, $E_{\text{neutron}}(\rho) = E_{\text{neutron}}(\rho_0) + L/3 (\rho - \rho_0)/\rho_0$ where L is related to the derivative of the nuclear symmetry energy. The inset in Fig. 1 shows the correlation between E_{sym} and L . This correlation is insensitive to the large variations in the range of the short-range 3n force μ and the strength of the 3π term $A_{3\pi}$. This is in sharp contrast to the pre-

dictions of mean field theories where the slope was found to be very sensitive to the choice of effective interactions [27]. Previous calculations of neutron matter up to ρ_0 [28] use a chiral 2n interaction fit to lab energies of 350 MeV plus the two-pion exchange three-nucleon interaction to calculate the neutron matter equation of state using perturbation theory. In contrast to our results, they find a significant repulsion from the 2π exchange long range 3n interaction. Since this force is better constrained by light nuclei, they can make a prediction for the neutron matter energy independent of the phenomenological short-range interaction that plays an important role in our calculation. To understand this basic difference further tests of the convergence of perturbation theory and the chiral expansion in the diagrammatic calculations, a survey of other two-body interactions in the AFDMC, and the incorporation of chiral interactions in non-perturbative methods such as lattice and suitable extension of QMC would be necessary.

Current determinations of L have relied on analysis of neutron-skins, surface contributions to the symmetry energy of neutron-rich nuclei, and isospin diffusion in heavy-ion reactions. These studies have been useful, but not very constraining as acceptable values are in the range $L = 40 - 100$ MeV[25]. However, a better determination of L even with modest reduction in the error would test our model for 2n and 3n interactions.

The predictions of QMC can be accurately fit using

$$E(\rho) = a \left(\frac{\rho}{\rho_0} \right)^\alpha + b \left(\frac{\rho}{\rho_0} \right)^\beta, \quad (3)$$

where the coefficients a and α are sensitive to the low density behavior of the EoS, while b and β are sensitive to the high density physics [29]. We find that the 3n force plays a key role in determining the coefficient b and the variation of the other EoS parameters is comparatively small. Numerical values for these parameters are reported in Tab. I for selected Hamiltonians.

3N force	E_{sym} (MeV)	L (MeV)	a (MeV)	α	b (MeV)	β
none	30.5	31.3	12.7	0.49	1.78	2.26
$V_{2\pi}^{PW} + V_{\mu=150}^R$	32.1	40.8	12.7	0.48	3.45	2.12
$V_{2\pi}^{PW} + V_{\mu=300}^R$	32.0	40.6	12.8	0.488	3.19	2.20
$V_{3\pi} + V_R$	32.0	44.0	13.0	0.49	3.21	2.47
$V_{2\pi}^{PW} + V_{\mu=150}^R$	33.7	51.5	12.6	0.475	5.16	2.12
$V_{3\pi} + V_R$	33.8	56.2	13.0	0.50	4.71	2.49
UIX	35.1	63.6	13.4	0.514	5.62	2.436

TABLE I. Fitting parameters for the neutron matter EoS defined in Eq. 3 for selected different Hamiltonians.

To calculate the mass and radius of neutron stars we solve the Tolman-Oppenheimer-Volkoff (TOV) equations for the hydrostatic structure of a spherical non-rotating star using the QMC equation of state for neutron matter [30, 31]. The QMC EoS is used for $\rho \geq \rho_{\text{crust}} = 0.08$

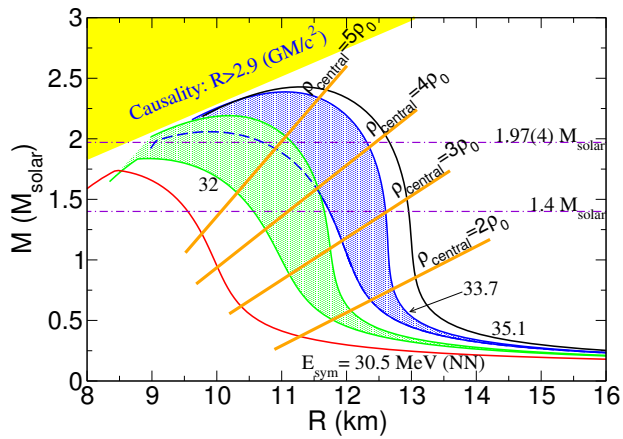


FIG. 2. (Color online) Mass-Radius relation for the EoS with three-neutron interactions corresponding to the bands for different E_{sym} shown in Fig. 1. The intersection with the orange lines roughly indicate central densities realized in these stars.

fm^{-3} . Below this density we use the EoS of the crust obtained in earlier works in Ref. [32] and [33].

The neutron star mass-radius predictions are obtained by varying the $3n$ force and shown in Fig. 2. The striking feature is the estimated error in the neutron star radius with a canonical mass of $1.4 M_{\text{solar}}$. The uncertainty in the measured symmetry energy of ± 2 MeV leads to an uncertainty of about 3 km for the radius, while the uncertainties in the short-distance structure of the $3n$ force predicts a radius uncertainty of $\lesssim 1$ km. The different bands of Fig. 2 correspond to EoS of Fig. 1 with the same colors, giving different values of E_{sym} .

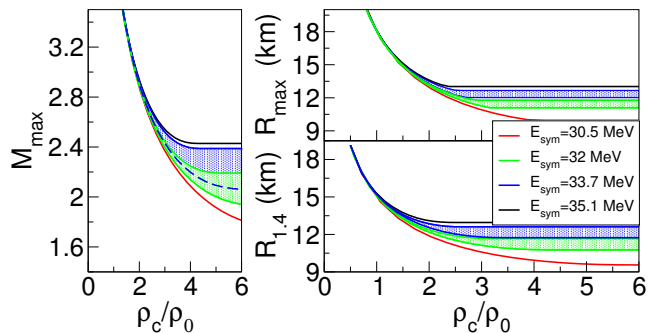


FIG. 3. (Color online) Bounds on the maximum mass and radius for different equations of state as a function of the critical density ρ_c . The left panel shows the maximum mass, the right top and bottom panels shows the maximum possible radius for any neutron star with mass greater than $1.2 M_{\text{solar}}$ and for a neutron star with $M = 1.4 M_{\text{solar}}$, respectively.

The central density of stars $M \gtrsim 1.5 M_{\text{solar}}$ are larger than $3\rho_0$. At these higher densities, the effects such as relativistic corrections to the kinetic energy, retardation effects in the potential, and 4- and higher body forces become important. Consequently, non-relativistic models violate causality and predict a sound speed $c_s =$

$\sqrt{\partial p / \partial \epsilon} \gtrsim c$ for $\rho \simeq 4 - 5\rho_0$. To overcome this deficiency we adopt the strategy suggested in Ref. [34] and replace the EoS above a critical density ρ_c by the maximally stiff or causal EoS given by $p(\epsilon) = c^2 \epsilon - \epsilon_c$, where p is the pressure, ϵ is the energy density, c is the speed of light and ϵ_c is a constant. This EoS is maximally stiff and predicts the most rapid increase of pressure with energy density without violating causality. The constant ϵ_c is the parameter that determines the discontinuity in energy density between the low and high density EoS's. Our choice of ϵ_c ensures that the energy density is continuous and provides an upper bound on both the radius and the maximum mass of the neutron star.

Fig. 3 shows how the bound on the maximum radius and mass of the neutron star vary with our choice of the critical density ρ_c . It also illustrates that the bounds provide useful constraints only when the EoS is known up to $2 - 3 \rho_0$. In Ref. [35] bounds on the radius were derived by using an EoS of neutron matter calculated up to ρ_0 with specific assumptions about polytropic equations of state at higher densities. Our upperbounds are model independent and show that the radius of $1.4 M_{\text{solar}}$ can be as large as 16 km if $\rho_c = \rho_0$. To obtain a tighter bound the equation of state between $1 - 2\rho_0$ is important. The red, green, blue and black curves are predictions corresponding to the $3n$ interaction strength fit to $E_{\text{sym}} = 30.5, 32.0, 33.7$ and 35.1 MeV, respectively. We also note that these bounds do not change much for $\rho_c \gtrsim 4\rho_0$ because the QMC EoS is already close to being maximally stiff in this region. These upper bounds provide a direct relation between the experimentally measurable nuclear symmetry energy and the maximum possible mass and radius of neutron stars.

To summarize, we predict that the correlation between the symmetry energy and its derivative at nuclear density is nearly independent of the detailed short-range $3n$ force once its strength is tuned to give a particular value of E_{sym} . Consequently, in our model one short-distance parameter A_R completely determines the behavior of the EoS. At higher density, the sensitivity to short-distance behavior of the $3n$ interaction translate to an uncertainty of about 1 km for the neutron star radius with mass $M = 1.4 M_{\text{solar}}$. While the uncertainty at high density due to a poorly constrained symmetry energy is larger $\simeq 3$ km. Within our model we predict that neutron star radii are in the 10–13 km for nuclear symmetry energy in the range 32–34 MeV. If nuclear experiments can determine that $E_{\text{sym}} \leq 32$ MeV, QMC predicts that $L \lesssim 45$ MeV at nuclear density, and for neutron stars it predicts $M_{\text{max}} < 2.2 M_{\text{solar}}$ and $R < 12$ km for a neutron star with $M = 1.4 M_{\text{solar}}$. The relationship between the symmetry energy and its density dependence is experimentally relevant, and its implications on the neutron star mass radius relationship are subject to clear observational tests.

We thank Bob Wiringa, Steve Pieper, Kevin Schmidt and Francesco Pederiva, for useful discussions. We also thank Chuck Horowitz, Jim Lattimer, Madappa Prakash, and Achim Schwenk for comments on an early ver-

sion of the manuscript. This work was supported by a grant from the Department of Energy (DOE) under contracts DE-FC02-07ER41457 (UNEDF SciDAC), DE-AC52-06NA25396 (LANL), and the DOE topical collaboration to study "Neutrinos and nucleosynthesis in hot

and dense matter". Computer time was made available by Los Alamos Open Supercomputing, and by the National Energy Research Scientific Computing Center (NERSC).

-
- [1] P. B. Demorest, T. Pennucci, S. M. Ransom, M. S. E. Roberts, and J. W. T. Hessels, *Nature* **467**, 1081 (2010).
- [2] N. A. Webb and D. Barret, *Astrophys. J.* **671**, 727 (2007).
- [3] T. Güver, P. Wroblewski, L. Camarota, and F. Özel, *Astrophys. J.* **719**, 1807 (2010).
- [4] A. W. Steiner, J. M. Lattimer, and E. F. Brown, *Astrophys. J.* **722**, 33 (2010).
- [5] S. C. Pieper, V. R. Pandharipande, R. B. Wiringa, and J. Carlson, *Phys. Rev. C* **64**, 014001 (2001).
- [6] A. W. Steiner, M. Prakash, J. M. Lattimer, and P. J. Ellis, *Phys. Rep.* **411**, 325 (2005).
- [7] D. V. Shetty, S. J. Yennello, and G. A. Souliotis, *Phys. Rev. C* **76**, 024606 (2007).
- [8] K. E. Schmidt and S. Fantoni, *Phys. Lett. B* **446**, 99 (1999).
- [9] S. Gandolfi, F. Pederiva, S. Fantoni, and K. E. Schmidt, *Phys. Rev. Lett.* **99**, 022507 (2007).
- [10] A. Sarsa, S. Fantoni, K. E. Schmidt, and F. Pederiva, *Phys. Rev. C* **68**, 024308 (2003).
- [11] S. Gandolfi, J. Carlson, and S. C. Pieper, *Phys. Rev. Lett.* **106**, 012501 (2011).
- [12] J. M. Lattimer and M. Prakash, *Astrophys. J.* **550**, 426 (2001).
- [13] R. B. Wiringa, V. G. J. Stoks, and R. Schiavilla, *Phys. Rev. C* **51**, 38 (1995).
- [14] R. B. Wiringa private Communication, <http://www.phy.anl.gov/theory/research/av18/>.
- [15] R. Schiavilla, R. B. Wiringa, S. C. Pieper, and J. Carlson, *Phys. Rev. Lett.* **98**, 132501 (2007).
- [16] E. Piasezky, M. Sargsian, L. Frankfurt, M. Strikman, and J. W. Watson, *Phys. Rev. Lett.* **97**, 162504 (2006).
- [17] A. Tang, J. W. Watson, J. Aclander, J. Alster, G. Asryan, Y. Averichev, D. Barton, V. Baturin, N. Bukhtoyarova, A. Carroll, S. Gushue, S. Heppelmann, A. Leksanov, Y. Makdisi, A. Malki, E. Minina, I. Navon, H. Nicholson, A. Ogawa, Y. Panebratsev, E. Piasezky, A. Schetkovsky, S. Shimanskiy, and D. Zhalov, *Phys. Rev. Lett.* **90**, 042301 (2003).
- [18] R. Subedi, R. Shneor, P. Monaghan, B. D. Anderson, K. Aniol, J. Annand, J. Arrington, H. Benaoum, F. Benmokhtar, W. Boeglin, J. Chen, S. Choi, E. Cisbani, B. Craver, G. Frullani, F. Garibaldi, S. Gilad, R. Gilman, O. Glamazdin, J. Hansen, D. W. Higinbotham, T. Holmstrom, H. Ibrahim, R. Igarashi, C. W. de Jager, E. Jans, X. Jiang, L. J. Kaufman, A. Kelleher, A. Kolarkar, G. Kumbartzki, J. J. LeRose, R. Lindgren, N. Liyanage, D. J. Margaziotis, P. Markowitz, S. Marrone, M. Mazouz, D. Meekins, R. Michaels, B. Moffit, C. F. Perdrisat, E. Piasezky, M. Potokar, V. Punjabi, Y. Qiang, J. Reinhold, G. Ron, G. Rosner, A. Saha, B. Sawatzky, A. Shahinyan, S. Širca, K. Slifer, P. Solvignon, V. Sulkosky, G. M. Urciuoli, E. Voutier, J. W. Watson, L. B. Weinstein, B. Wojtsekhowski, S. Wood, X. Zheng, and L. Zhu, *Science* **320**, 1476 (2008).
- [19] R. Shneor, P. Monaghan, R. Subedi, B. D. Anderson, K. Aniol, J. Annand, J. Arrington, H. Benaoum, F. Benmokhtar, P. Bertin, W. Bertozzi, W. Boeglin, J. P. Chen, S. Choi, E. Chudakov, E. Cisbani, B. Craver, C. W. de Jager, R. J. Feuerbach, S. Frullani, F. Garibaldi, O. Gayou, S. Gilad, R. Gilman, O. Glamazdin, J. Gomez, J. Hansen, D. W. Higinbotham, T. Holmstrom, H. Ibrahim, R. Igarashi, E. Jans, X. Jiang, Y. Jiang, L. Kaufman, A. Kelleher, A. Kolarkar, E. Kuchina, G. Kumbartzki, J. J. LeRose, R. Lindgren, N. Liyanage, D. J. Margaziotis, P. Markowitz, S. Marrone, M. Mazouz, D. Meekins, R. Michaels, B. Moffit, S. Nanda, C. F. Perdrisat, E. Piasezky, M. Potokar, V. Punjabi, Y. Qiang, J. Reinhold, B. Reitz, G. Ron, G. Rosner, A. Saha, B. Sawatzky, A. Shahinyan, S. Širca, K. Slifer, P. Solvignon, V. Sulkosky, N. Thompson, P. E. Ulmer, G. M. Urciuoli, E. Voutier, K. Wang, J. W. Watson, L. B. Weinstein, B. Wojtsekhowski, S. Wood, H. Yao, X. Zheng, and L. Zhu, *Phys. Rev. Lett.* **99**, 072501 (2007).
- [20] R. B. Wiringa and S. C. Pieper, *Phys. Rev. Lett.* **89**, 182501 (2002).
- [21] S. C. Pieper and R. B. Wiringa private Communication.
- [22] S. C. Pieper, *AIP Conf. Proc.* **1011**, 143 (2008).
- [23] A. Akmal, V. R. Pandharipande, and D. G. Ravenhall, *Phys. Rev. C* **58**, 1804 (1998).
- [24] E. Epelbaum, H. Hammer, and U. Meißner, *Rev. Mod. Phys.* **81**, 1773 (2009).
- [25] M. B. Tsang, Y. Zhang, P. Danielewicz, M. Famiano, Z. Li, W. G. Lynch, and A. W. Steiner, *Phys. Rev. Lett.* **102**, 122701 (2009).
- [26] P. Möller, J. R. Nix, W. D. Myers, and W. J. Swiatecki, *At. Data Nucl. Data Tables* **59**, 185 (1995).
- [27] B. Alex Brown, *Phys. Rev. Lett.* **85**, 5296 (Dec 2000).
- [28] K. Hebeler and A. Schwenk, *Phys. Rev. C* **82**, 014314 (2010).
- [29] S. Gandolfi, A. Y. Illarionov, K. E. Schmidt, F. Pederiva, and S. Fantoni, *Phys. Rev. C* **79**, 054005 (2009).
- [30] J. M. Lattimer and M. Prakash, *Science* **304**, 536 (2004).
- [31] S. Gandolfi, A. Y. Illarionov, S. Fantoni, J. Miller, F. Pederiva, and K. Schmidt, *Mon. Not. R. Astron. Soc.* **404**, L35 (2010).
- [32] G. Baym, C. Pethick, and P. Sutherland, *Astrophys. J.* **170**, 299 (1971).
- [33] J. W. Negele and D. Vautherin, *Nucl. Phys. A* **207**, 298 (1973).
- [34] C. E. Rhoades and R. Ruffini, *Phys. Rev. Lett.* **32**, 324 (1974).
- [35] K. Hebeler, J. M. Lattimer, C. J. Pethick, and A. Schwenk, *Phys. Rev. Lett.* **105**, 161102 (2010).